Journal of Luminescence 131 (2011) 1739–1746

Contents lists available at ScienceDirect

Journal of Luminescence

journal homepage: www.elsevier.com/locate/jlumin

The Frenkel exciton Hamiltonian for functionalized Ru(II)–bpy complexes

Victor V. Albert [a], Ekaterina Badaeva [b,a], Svetlana Kilina [a], Milan Sykora [c], Sergei Tretiak [a,*]

[a] Theoretical Division, Center for Nonlinear Studies (CNLS), and Center for Integrated Nanotechnologies (CINT), Los Alamos National Laboratory, Los Alamos, NM 87545, United States
[b] Department of Chemistry, University of Washington, Seattle, WA 98195, United States
[c] Chemistry Division, Los Alamos National Laboratory, Los Alamos, NM 87545, United States

ARTICLE INFO

Article history:
Received 31 August 2010
Received in revised form
31 March 2011
Accepted 4 April 2011
Available online 12 April 2011

Keywords:
DFT
TDDFT
Frenkel exciton model
Ru(bpy)
Functionalized pyridine

ABSTRACT

Electronic excitation energies and wavefunctions are calculated for $Ru(bpy)_3^{+2}$ (bpy = 2,2′-bipyridine) and its two derivatives, where one or two bpy ligands are functionalized with carboxyl and methyl groups. We show that the structure of these molecules allows one to express their excitations in terms of wavefunctions localized on individual ligands via the Frenkel exciton model. The model is based on three parameters – effective single-ligand excitation energy, inter-ligand interaction coupling, and energy shift brought by the ligand functionalization – that are extracted from time-dependent density functional theory (TDDFT). This simple model is able to accurately explain the optical intensity, localization properties, and splitting patterns of the low-energy excited states not only in molecules with a high degree of symmetry, but also in non-symmetrically functionalized Ru(II) complexes in vacuum and in solvent. Such reduced description of the excited states provides better understanding and interpretation of experimental data on Ru–polypyridine complexes, and allows for description of excited-state structure in a large ensemble of interacting molecules and treatment of possible charge and energy transfer phenomena in the material.

1. Introduction

The family of the $[Ru(bpy)_3]^{2+}$ (bpy = 2,2′-bipyridine) complex has been a long-standing area of research ever since the discovery that $[Ru(bpy)_3]^{2+}$ can act as a photosensitizer [1]. Since then, various other applications for the complexes have developed [2], including molecular electronics [3], artificial photosynthesis [4], photo-detectors and sensors [5], photochemical and photovoltaic cells [6–10], and molecular catalysts [11–13]. A characteristic feature of these compounds is the formation of metal-to-ligand charge transfer (MLCT) states: upon photo-excitation, the electron density redistributes from the central Ru donor to the three bpy acceptors. The MLCT states define the photophysical and redox properties of these complexes. When excited, $[Ru(bpy)_3]^{2+}$ becomes either an excellent electron donor or acceptor, depending on the specific circumstances [2,14], making it a very appealing sensitizer for solar energy conversion applications such as photovoltaics [6] and photocatalysis [12]. Therefore, the problem of assignment of the MLCT spectra and retrieval of detailed information about the structure and properties of the MLCT excited states has attracted a lot of attention both from experimental and theoretical sides.

Beginning in 1980, there has been considerable progress in analysis of the MLCT spectra of symmetric Ru-complexes [15–21] and analogous species [22–25] based on effective models incorporating MO and ligand-field theories. The parameters for these reduced Hamiltonian models such as orbital energies, exchange integrals, and spin–orbit coupling constants have been derived relying on symmetry considerations and a complex fit to the available spectroscopic data. These molecular orbital schemes and DFT calculations indeed work well for symmetric molecules such as $[Ru(bpy)_3]^{2+}$ [16,20,21]. However, their application is limited when the symmetry is broken, as is the case when one or two ligands are changed or substituted. Meanwhile, it is well recognized that chemical reactivity and redox, optical, and electronic properties of Ru(II) complexes can be tuned via modifications of peripheral ligands [26]. For example, in TiO_2-based photovoltaic devices (Grätzel cells), Ru(II) polypyridine complexes are used as sensitizers and the ligands are modified with one or more carboxyl functionalities to enable anchoring of the complex to the TiO_2 surface [27,28]. Similar functionalization of anchoring ligands is used in photo-electrochemical cells and catalyst agents based on colloidal quantum dots and Ru-complexes to provide a means for chemical and electronic coupling of the complexes to the quantum dot surface [8–10,29,30]. Modification of the non-anchoring ligands is also commonly used to tailor the absorption spectra of the complexes and enhance their light harvesting abilities [6,31]. It is thus of significant importance to quantify the effect of ligand functionalization on the optical properties of various Ru(II)-complexes.

To treat such cases, it is possible to use a simple Frenkel exciton model, which represents the excitation as a tightly bound

* Corresponding author. Tel.: +1 505 667 8351.
E-mail address: serg@lanl.gov (S. Tretiak).

0022-2313/$ - see front matter © 2011 Elsevier B.V. All rights reserved.
doi:10.1016/j.jlumin.2011.04.009

electron–hole pair localized on a part of a molecular structure, e.g., a single bpy ligand and a metal center. Compared to the previous efforts, this reduced parameterization is simpler, can be unambiguously extended for the case of asymmetric ligands, and has been previously applied to many molecular materials [32–38], thus providing a conceptually attractive common theoretical framework. Particularly, its parameters naturally emerge from electronic structure calculations (such as accurate time-dependent density functional theory, TDDFT, calculations) of specific molecular fragments, and can be further refined by using relevant spectroscopic data.

We have recently analyzed [39] changes in electronic structure and optical response of $[Ru(bpy)_3]^{2+}$ complexes that occur when the bpy ligands are functionalized with methyl groups and protonated/de-protonated carboxyl groups—a typical modification in photochemical cells. Pairing experimental excited-state studies with TDDFT modeling, we have found that addition of the carboxyl/methyl groups to $[Ru(bpy)_3]^{2+}$ red-shifts the MLCT absorption and emission bands due to stabilization of the lowest unoccupied orbitals localized on the substituted ligands [39].

In the present paper, we continue to study the same compounds: $[Ru(bpy)_3]^{2+}$, $[Ru(bpy)_2(mcb)]^{2+}$, and $[Ru(bpy)(mcb)_2]^{2+}$, where "bpy" = 2,2′-bipyridine and "mcb" = 4-carboxy-4′-methyl-2,2′-bipyridine, which are abbreviated as **C1**, **C2**, and **C3**, respectively (Fig. 1). The aim of this work is to test the applicability of the Frenkel exciton model [34,40,41] not only for the pristine **C1**, but more importantly for its non-symmetric functionalized derivatives **C2** and **C3**. Based on parameters from TDDFT calculations, this simple model allows one to determine the predominant factors affecting optical intensity and splitting patterns of the low-energy excited states of Ru(II) complexes as well as quantify the interactions between the ligands. We also demonstrate that the Frenkel model adequately describes energetics of electronic excitations of Ru(II) complexes in vacuum and in a solvent environment, predicting and explaining experimentally observed trends of absorption red-shifts and localization of the lowest energy excitation on the substituted ligands. This parameterization potentially permits treatment of electronic phenomena in large assemblies of interacting molecules, for example, relevant to photovoltaic device architectures [7,8,27–30]. The manuscript is organized as follows: We introduce the Frenkel exciton Hamiltonian in Section 2, discuss details of quantum-chemical calculation in Section 3, and demonstrate an application to three different Ru–polypyridine complexes in a gas phase and in a solvent environment in Section 4. Finally, Section 5 summarizes our results and observed trends.

2. Frenkel exciton model

In a Frenkel, or molecular, exciton, the electron and its corresponding hole are tightly coupled and are thus localized on a part of a molecular structure that can be thought of as a "sub-unit" or a "branch" (usually a molecule) [34,40,41]. This is different from the Wannier exciton limit, where the electron and hole are loosely coupled and tend to be delocalized or "diffused" throughout the entire molecular structure [42]. Typical examples of Frenkel excitons are alkalihalide crystals and organic molecular crystals composed of aromatic molecules [41], where the orbital overlap between molecules is small and an intermolecular interaction is of electrostatic nature (dipole–dipole coupling being the simplest case). In its simplest form, the Frenkel exciton Hamiltonian describes a weakly interacting ensemble of two-level systems:

$$H = \sum_{i=1} \Omega_i b_i^{\dagger} b_i + \sum_{i \neq j} s_{ij} (b_i^{\dagger} b_j + b_j b_i^{\dagger}), \quad (1)$$

where indices i and j label "sub-units" (molecules), $b_i^{\dagger}$ (b_i) are creation (annihilation) operators of an excitation on molecule i, Ω_i is the excited-state transition energy of molecule i, and s_{ij} is the electrostatic interaction, or coupling, between molecules i and j. This model serves as a basis for more sophisticated theoretical

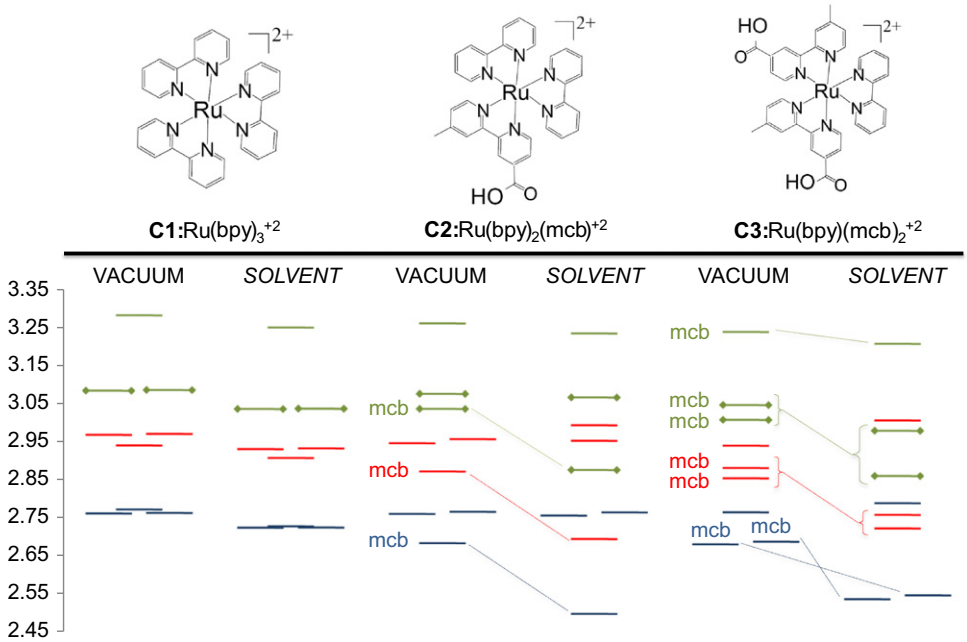

Fig. 1. Chemical structures (top) and the first nine excited-state energies (eV) of the studied Ru(II)-polypyridine complexes calculated by TD-B3LYP in vacuum and in solvent. Bands I, II, and III are colored blue, red, and green, respectively. The green capped bars represent the bright excited states with oscillator strength ≥ 0.10. The "mcb" label is next to those states whose orbitals are significantly localized on one of the bipyridine ligands functionalized with carboxyl and methyl groups (mcb-π^* orbitals). The dashed lines show the red-shift that occurs in solution because of the stronger stabilization of the mcb-π^* orbitals, which mixes the Frenkel bands. Overall, substitution of mcb ligands results in the red-shift of excited energies both in vacuum and in solvent. (For interpretation of the references to color in this figure legend, the reader is referred to the web version of this article.)

frameworks that have been used extensively in the past to describe electronic structure and spectroscopic properties of many molecular materials such as organic molecular crystals [41,43], various J- and H-aggregates [35,44–46], biological light-harvesting complexes [36,47–50], self-assembled systems [37,51], etc. Notably that this approach remains robust in several cases when neighboring "sub-units" share a common part of the molecular structure such as dendrimeric [32,33,52–54] and branching structures [55–59]. In these example, while orbital overlap may not be vanishing, still it produces interactions between "sub-units" being small compared to the electrostatic Coulomb coupling. Finally, the Frenkel exciton based modeling can be conveniently extended to incorporate vibrational interactions [35,60] and even an effect of charge-transfer excitonic bands [61].

In a related example to the model we use, Terenziani et al. [55] studied several types of branched chromophores consisting of conjugated chains and a nitrogen atom branching center and showed that the Frenkel model can be used to connect photophysical properties of branched chromophores to their monomeric counterparts. A very interesting conclusion of the above work is that the Frenkel exciton model accurately describes the energetics of the excitations in this system, although the excitons are not really localized on the polymer branches since the nitrogen center also contributes to the excitation. Similarly, compound **C1** can be treated as a symmetric combination of three bipyridine ligands connected through the Ru center. For low-energy MLCT excited states, the hole is localized on the ruthenium with a small contribution from ligands while the electron wavefunction is localized on the ligands [39]. Consequently, the Hamiltonian (1) for **C1** in the ligand-localized basis becomes

$$H=\begin{pmatrix} \Omega & s & s \\ s & \Omega & s \\ s & s & \Omega \end{pmatrix}, \tag{2}$$

where $\Omega_i=\Omega$ since all ligands are identical and the molecule has D_3 symmetry in the case of **C1** (which is confirmed by quantum-chemical calculations). Note that Ω_i is not the real excitation energy of the pristine bipyridine molecule, since the effective energy also includes effects of the Ru donor. Due to the D_3 symmetry, all inter-ligand couplings are also the same and real-valued ($s_{ij}\cong s$). The latter will be assumed from now on for all complexes we study.

The eigenvalues of the Hamiltonian in Eq. (2), represented as $\{E_i\}$ in Tables 1 and 2, correspond to the group of three excited-state transition energies of the Ru complex are $\{\Omega-s,\Omega-s,\Omega+2s\}$. Their order is determined by the sign of s, as shown in the two columns left of the gray arrow in Fig. 2(a). Owing to the pseudo-octahedral coordination field of the bpy ligands (D_3 symmetry), the lowest excitations obtained from TDDFT can be combined into groups of three, denoted further in the text and figures as bands I, II, III, etc. Setting the three eigenvalues of Eq. (2) equal to the TDDFT energies of the three excited states of each band in vacuum, we can determine the values of Ω and s, presented in Table 1. Note that because the Frenkel excitons are localized on a single ligand, the coupling term

Table 1
Excited-state energies (eV) calculated by TD-B3LYP in vacuum and parameters (eV) of the deduced effective Frenkel exciton Hamiltonian for the first three bands of excited states of **C1**, **C2**, and **C3**. Each of the three excitation energies of each band is separated by slashes. Bright excited states with oscillator strengths >0.1 are highlighted in bold.

Band	Parameters	**C1**	**C2**	**C3**
I	$E_1/E_2/E_3$	2.76/2.76/2.77	2.69/2.76/2.77	2.68/2.69/2.77
	Ω	2.76	2.76	2.77
	ε		0.07	0.08
	s	0.003	0.005	0.005
II	$E_4/E_5/E_6$	2.94/2.97/2.97	2.87/2.95/2.96	2.86/2.88/2.94
	Ω	2.96	2.95	2.94
	ε		0.08	0.07
	s	−0.010	−0.005	−0.009
III	$E_7/E_8/E_9$	**3.09**/**3.09**/3.28	**3.04**/**3.08**/3.26	**3.01**/**3.05**/3.24
	Ω	3.15	3.15	3.15
	ε		0.06	0.07
	s	0.063	0.065	0.067

Table 2
Excited-state energies (eV) calculated by TD-B3LYP in solution and parameters (eV) of the deduced effective Frenkel Hamiltonian model for the first three re-organized bands of excited states of **C1**, **C2**, and **C3**. Each of the three excitation energies of each band is separated by slashes. Bright excited states with oscillator strengths >0.1 are highlighted in bold.

	Parameters	**C1**	**C2**	**C3**
I	$E_1/E_2/E_3$	2.73/2.73/2.73	2.50/2.76/2.77	2.54/2.55/2.79
	Ω	2.73	2.76	2.79
	ε		0.26	0.24
	s	0	0.005	0.005
II	$E_4/E_5/E_6$	2.91/2.93/2.93	2.70/2.95/3.00	2.72/2.76/3.01
	Ω	2.92	2.97	3.01
	ε		0.26	0.27
	s	−0.007	−0.028	−0.019
III	$E_7/E_8/E_9$	**3.04**/**3.04**/3.25	**2.88**/**3.07**/3.24	**2.86**/**2.98**/3.21
	Ω	3.11	3.14	3.19
	ε		0.23	0.26
	s	0.070	0.070	−0.052

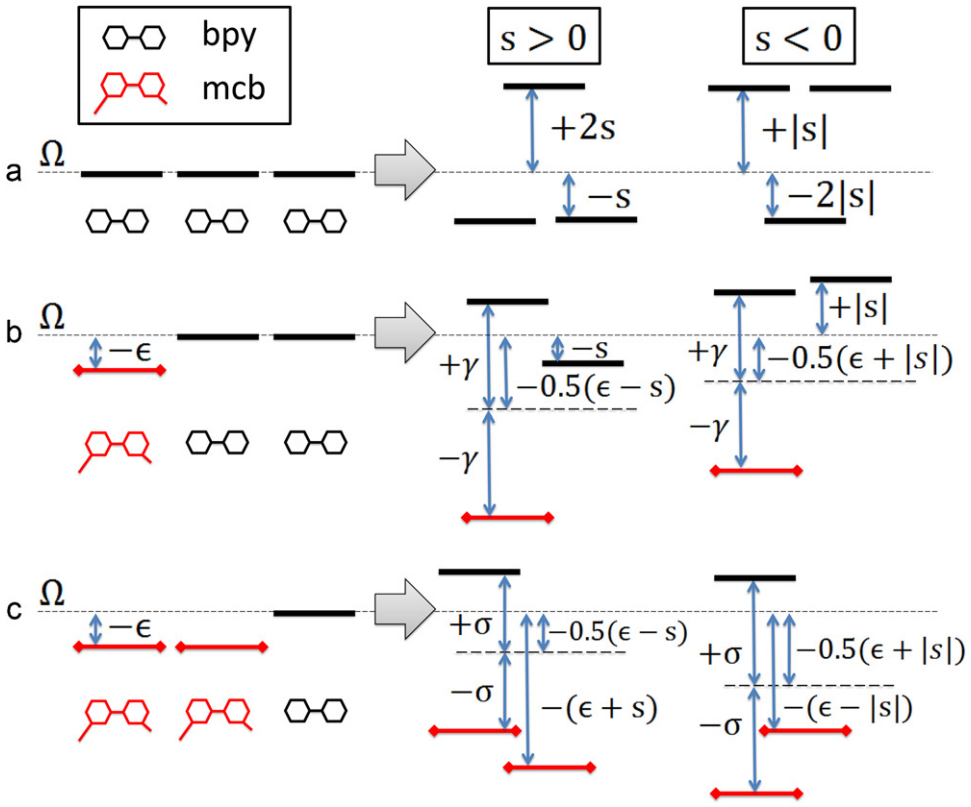

Fig. 2. Schematic electronic level diagrams within the Frenkel exciton model for **C1** (a), **C2** (b), and **C3** (c). The effective energies of the lowest excited states for each isolated ligand, Ω and $\Omega-\varepsilon$, are depicted left of the gray arrow. The excitation energies of each complex are represented in terms of the parameters Ω, ε, and s and depicted right of the arrow. These diagrams show the relative order of the three excitations energies (solid lines). There is only one degree of freedom in the sign of s (since we restricted ε to be positive) and thus two possibilities of state ordering, $s>0$ (left column) and $s<0$ (right column). The values $\gamma(\pm|s|)=\frac{1}{2}\sqrt{9s^2\pm 2\varepsilon|s|+\varepsilon^2}$ and $\sigma(\pm|s|)=\frac{1}{2}\sqrt{9s^2\mp 2\varepsilon|s|+\varepsilon^2}$, as obtained from the eigenvalue solution of the Frenkel Hamiltonian.We note that the placement of the solid lines with respect to the baseline Ω (short dashes) and splitting lines (long dashes) is not to scale and depend on the more specific relationships between s and ε.

between the ligands is necessarily much smaller than the effective single-ligand excited energies ($|s| \ll \Omega$) for all complexes. Thus, the inter-ligand coupling should be considered as a small perturbation to the system.

When a different ligand is substituted for one or two bipyridines (**C2** and **C3**, respectively), the Frenkel exciton Hamiltonian adopts the form:

$$H=\begin{pmatrix} \Omega-\varepsilon & s & s \\ s & \Omega-\varepsilon_1 & s \\ s & s & \Omega \end{pmatrix}. \tag{3}$$

For **C2**, $\varepsilon_1=0$ and for **C3**, $\varepsilon_1=\varepsilon$. The value ε is the energy displacement caused by substitution of mcb for a bpy ligand and constitutes a third parameter in our model. The Hamiltonian in Eq. (3) has three distinct eigenvalues: $\{\Omega-s,\Omega-\frac{1}{2}(\varepsilon-s)\pm\frac{1}{2}\sqrt{9s^2+2s\varepsilon+\varepsilon^2}\}$ for **C2** and $\{\Omega-(s+\varepsilon),\Omega-\frac{1}{2}(\varepsilon-s)\pm\frac{1}{2}\sqrt{9s^2-2s\varepsilon+\varepsilon^2}\}$ for **C3**. In the general case, we have two degrees of freedom in the signs of ε and s. However, it is well known that addition of an electron-withdrawing group (COOH) to an isolated bpy ligand decreases its excited-state energy. Therefore, it is reasonable to assume that the effective single-ligand energy of the substituted mcb ligand ($\Omega-\varepsilon$) should be smaller than that of the bpy ligand (Ω), leaving us with $\varepsilon>0$. We now have only two possible permutations of the eigenvalues depending on the sign of s, as illustrated in Figs. 2(b) and (c). The sign of s can be interpreted to determine whether there is attraction (+) or repulsion (−) between the ligands and depends on the spacial distribution of the wavefunction density on each ligand. Because the coupling s is a small perturbation, it is reasonable to assume that inter-ligand repulsion or attraction is only slightly perturbed by the substitution of bpy with mcb ligands. Thus the sign of s stays the same as it does in **C1** (Table 1): positive for bands I and III and negative for band II.

3. Computational details

The Gaussian09 [62] quantum chemistry software package is utilized to obtain optimal geometries and excited states in vacuum and in solvent. We use *acetonitrile* (CH_3CN; dielectric constant of 35.688) as the solvent. For our data presented in solvent, geometries of all complexes are optimized using the PCM solvation model [63,64], as implemented in Gaussian09. All TDDFT procedures are performed similar to those described in Ref. [39], namely using the hybrid B3LYP functional, the LANL2DZ basis set for Ru, and the 6-31G* basis set for the ligand atoms. This combination of functional and basis has been one of the most "tried-and-true" methods for calculating properties of Ru–polypyridine complexes, reproducing absorption spectra in past studies of similar systems [39,65–67]. However, while our previous work discusses how various solvation models can lead to different ground state orbital energies (Fig. 3 in Ref. [39]), these differing methods produce practically identical population densities of the excited states (shown in Fig. 4 of this work) and thus are not a factor in our calculations and analysis.

To illustrate the results, the Gaussian03 [68] suite is used for calculations of natural transition orbitals (NTOs) [69] for our complexes. NTO calculations offer the most compact representation of the transition density between the ground and excited states in terms of an expansion into single-particle transitions (hole and electron states for each given excitation). Here, we refer to the

unoccupied and occupied NTOs as "electron" and "hole" transition orbitals, respectively. Note that NTOs are not the same as virtual and occupied molecular orbital (MO) pairs from the ground state calculations. TDDFT transition density matrix typically mixes several pairs of the ground state MOs due to electronic correlation effects, while this quantity decomposes into a single pair of NTOs ("electron" and "hole" orbitals) in the most cases. All NTOs shown in this paper were produced with an orbital isovalue of 0.02 and visualized with the GaussView 4.1 interface [70].

4. Results and discussion

4.1. Excited-state energies and coupling constants

The energies of the first three excited bands, shown in Fig. 1, and the parameters of the Frenkel model, Ω, ε, and s, are listed in Table 1 for all three complexes. For the symmetric complex **C1** in vacuum, the first band consists of the lowest two transitions with a degenerate energy of 2.76 eV and the third transition with the slightly higher energy of 2.77 eV. Solution of the eigenvalue problem of Eq. (2) predicts the splitting between these states to be equal to $3s$. The inter-ligand coupling is positive for the first band, $s=0.003$ eV, as schematically represented in Fig. 2(a). However, the relative position of the degenerate and non-degenerate states is reversed in band II, resulting in a negative coupling: $s=-0.01$ eV. The coupling becomes positive again in band III: $s=0.063$ eV. Similar splitting of the excited-state energies into bands of three is also found for higher energy states generally following the behavior of the first three bands. While higher bands do not necessarily consist of MLCT transitions, the organization into bands remains most likely due to the symmetry of the ligands in this complex. The coupling is positive for both bands III and IV, demonstrating that the sign of s is not necessary alternating every band. As was previously discussed [39], the splitting between transitions and, consequently, the sign and the magnitude of the coupling s strongly correlate with redistribution of the charge density for each optical transition (delocalization of transition orbitals) over the bipyridine ligands in the complex.

Starting from a very small value, the coupling increases in magnitude from band I to band III. The coupling reaches the maximum value for band III, where there are two optically allowed, i.e., "bright," degenerate transitions (marked **bold** in Table 1). Such an increase in the coupling s for optically active band III can be attributed to strong Coulombic interactions between transition densities delocalized on ligands (i.e., significant dipole–dipole interaction as the first order term being large due to substantial transition dipole moments contributing to the oscillator strength of the optical transition). In contrast, the couplings are small for transitions with vanishing or very small transition dipole moments, i.e., "dark" transitions [39]. The overall trend signifies the conventional picture of the Frenkel exciton model that the coupling s, although relatively weak, is predominantly electrostatic and defines the excited-state fine structure.

Our calculations are comparable to results for **C1** reported earlier in Refs. [16,20,21]. In these in-depth theoretical approaches, Hamiltonian parameters for **C1** include not only inter-ligand but also spin–orbit (SO) couplings and are parametrized based on experimental data. In contrast to our approach relying on TDDFT simulations, these models analyze both excited singlet and triplet states based on combinations of ground state frontier orbitals, i.e., three occupied and three unoccupied electronic levels of **C1** in its ground state. According to Daul et al. [21], the difference between the energies associated with the first bright excitation and the next dark singlet transition in the calculated absorption spectra (21.86 and 23.22 cm^{-1} in Table 6 [21]) divided by three (since the splitting between these transitions is $3s$) results in the inter-ligand coupling $s\sim0.056$ eV for band III. Similarly, $s\sim0.087$ eV for the optically active band III can be extracted from the work of Kober and Meyer [20]. Our coupling for band III is 0.063 eV, which is comparable to the two previous models. Moreover, the spin–orbit coupling constants (e.g., 1200 cm^{-1} for $Ru(bpy)_3^{+2}$ ion [20]) can be further added to our model as additional variables following prescriptions developed before [16,20,21].

Beyond the symmetric system **C1**, our calculations based on the Frenkel model demonstrate reasonable and robust parameters s, Ω, and ε for the functionalized complexes **C2** and **C3** in vacuum, as shown in Table 1. For the functionalized complexes, the presence of one or two carboxyl groups on the bipyridine ligands (mcb) breaks the degeneracy of excited states and strongly stabilizes the energy of the states whose transition density is mostly localized on the substituted mcb ligands [39], as illustrated in Figs. 1 and 2(b) and (c). Nonetheless, for all three bands, the results for both **C2** and **C3** produce values of s very close to the coupling of **C1**. Such similarity in s values means that functionalization insignificantly affects the coupling between the ligands.

In all complexes, bands I and II are optically forbidden. The first two states in band III are the most optically active (shown in **bold** in Table 1) and demonstrate the largest values of the inter-ligand coupling s among all other low-energy transitions in complexes we study. The interactions between the ligands for excitations in band III are facilitated by the large transition dipole moments which provide a stronger optical response compared to that of bands I and II. Thus, the interaction parameter s of the Frenkel model can successfully predict the energetics and optical intensity of the low-energy excited states not only in pristine **C1**, but also in the functionalized complexes. Below we show how all three Frenkel parameters correlate with splitting patterns and localization properties of low-energy excitations.

4.2. Transition orbitals and eigenvectors of the Frenkel Hamiltonian

In a previous work [39], we have demonstrated that each excited state can be well-represented as an excitation between a single dominant pair consisting of the occupied (hole) natural transition orbital and the unoccupied (electron) natural transition orbital. Thus, we can analyze the NTO localization properties and compare them with the eigenfunctions of the Frenkel Hamiltonian.

The first band of electron NTOs for both pristine and functionalized complexes is shown in Fig. 3. Since the hole NTOs are mainly located on the Ru atom [39], these do not vary from state-to-state and, therefore, are not shown. Each respective eigenfunction of the Hamiltonian is listed below the NTO in Fig. 3. The eigenfunctions are represented in the ligand basis $|lig_i\rangle$, where i is the number of the ligand listed counterclockwise from the top. For example, the third transition of **C2** corresponds to the Frenkel eigenfunction $(0.08,0.7,0.7)=0.08|lig_1\rangle+0.70|lig_2\rangle+0.70|lig_3\rangle$. Counterclockwise from the top of the picture, the first ligand is mcb, while the other two are bpy. Therefore, the third transition of band I of **C2** is mostly localized on the un-substituted bipyridines with a negligible contribution from the functionalized mcb ligand, which is in excellent agreement with the electron NTO of this state.

Overall, the predicted eigenfunctions correspond well to the transition orbitals in Fig. 3. For all functionalized complexes, both NTOs and Frenkel eigenfunctions demonstrate localization of the lowest orbitals of band I on the mcb ligands with the higher energy transitions localized on the un-substituted bipyridines. Figs. 2(b) and (c) schematically explain this trend. The addition of the carboxyl, a weak electron–donor, and methyl groups to the isolated bipyridine

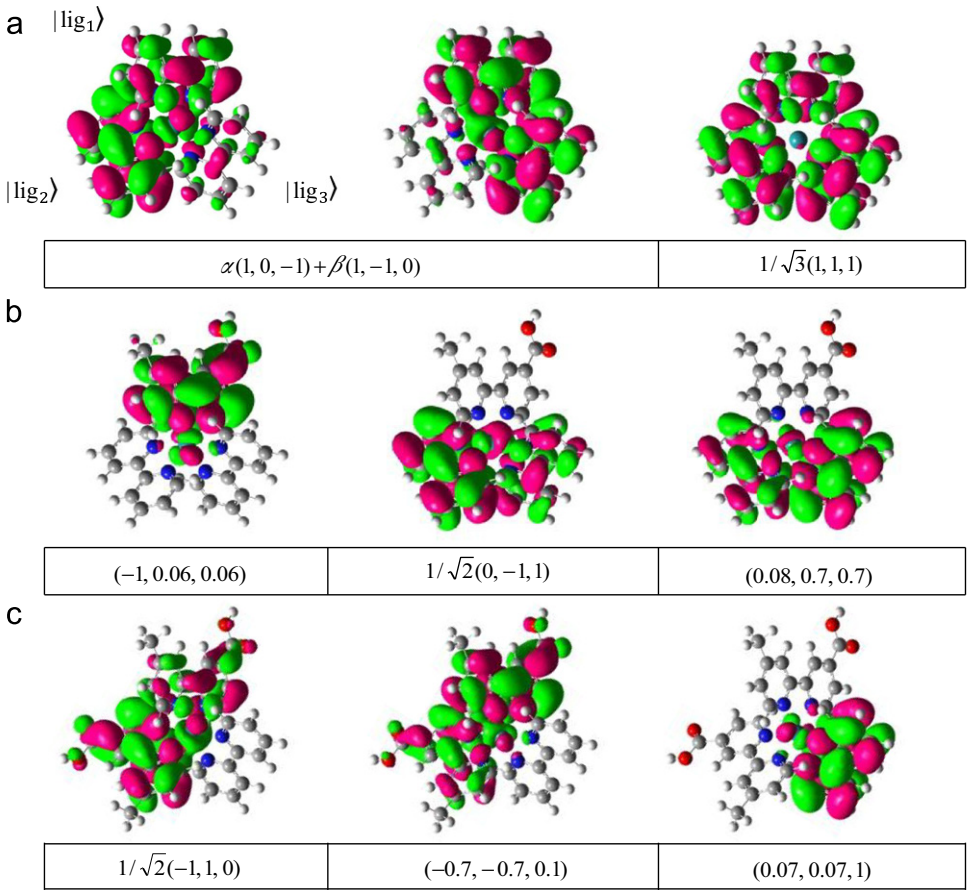

Fig. 3. Electron natural transition orbitals (NTOs) for band I of excited states of **C1** (a), **C2** (b), and **C3** (c) in vacuum. Each eigenfunction of the Frenkel Hamiltonian is shown below the orbital in the basis of individual ligands. The ligands are labeled counterclockwise from the top, i.e., state $|\mathrm{lig}_1\rangle$ is the top ligand, state $|\mathrm{lig}_2\rangle$ is the lower left, and $|\mathrm{lig}_3\rangle$ is the lower right. The eigenspace of **C1** is twofold degenerate and thus the first two orbitals can be any linear superposition of the two vectors listed with normalized coefficients α and β. Frenkel eigenfunctions show the analogous distribution of the wavefunction density over ligands as NTOs obtained from TD-B3LYP calculations.

ligand generally decreases the energy of the mcb ligand Ω by a positive ε. In these complexes, the mcb NTOs experience a stronger decrease in energy when compared to NTOs localized on bpy ligands, as followed from the solution to the eigenvalue problem of Eq. (3). Such a trend is observed for all bands, including optically active band III, and thus explains the red-shifts in the absorption spectra of functionalized complexes **C2** and **C3** when compared to pristine **C1** [39].

Competition between the inter-ligand coupling s and diagonal disorder ε is an important factor in determining whether the electron NTO is delocalized over all three ligands or localized on just one or two. When their magnitudes are of different (similar) order, the orbitals are localized (delocalized). From Table 1, $s \ll \varepsilon$ by about one order of magnitude for bands I and II. Consequently, mixing of orbitals between all three ligands is suppressed and transition orbitals have a more localized character due to very weak inter-ligand interactions. The localized character of excitations in bands I and II, including localization of the lower-energy transitions on the mcb and higher energy transitions on one or both of the bpy ligands, is clearly seen from electron NTOs of complexes **C2** and **C3** presented in Fig. 4. In contrast to bands I and II, the values of s and ε are of the same order in band III. Consequently, band III, as opposed to I and II, contains other significant orbitals (not shown) which exhibit a more delocalized character. Thus a simple Frenkel model not only explains the red-shifts in absorption spectra of functionalized Ru-complexes, but also correctly predicts the localization/delocalization properties of their low-energy excitations in vacuum.

4.3. Solvent effects

We have shown that the Frenkel model based on three parameters (s, Ω and ε) can describe both pristine and functionalized Ru-bipyridine complexes in vacuum. Here we analyze results of this model when solvation effects are introduced. The calculated absorption spectra of different Ru–polypyridine complexes are red-shifted in solution with respect to calculations in vacuum [39,71–74] (e.g., the excited-state energies of **C1**–**C3** have red-shifts in solvent, Fig. 1). However, for functionalized complexes **C2** and **C3**, the energy shift for transitions localized on mcb and bpy ligands is much more pronounced, resulting in significant mixing and overlaps of the original bands I, II, and III. The red-shift is largest for excitations localized on mcb ligands since those are most effectively stabilized by the electron-withdrawing carboxyl groups. In contrast, the energies for excited states localized on bpy ligands are not as significantly affected by solvent. It is possible to re-arrange the energies and reconstruct the original Frenkel bands by matching the transition orbitals in solution to their counterparts in vacuum. This matching, shown in Fig. 4 for complexes **C2** and **C3**, follows two sequential rules: (1) bright states in solution are matched to bright states in vacuum based on the magnitudes of their oscillator strengths and (2) remaining states are matched based on similarities in electron and hole (not shown) orbital symmetry and localization on specific ligands. Note that a few excitations of **C3** deviate from rule (2): the orbitals in solution and their vacuum counterparts look slightly different and are marked by dashed arrows in Fig. 4(b). This is

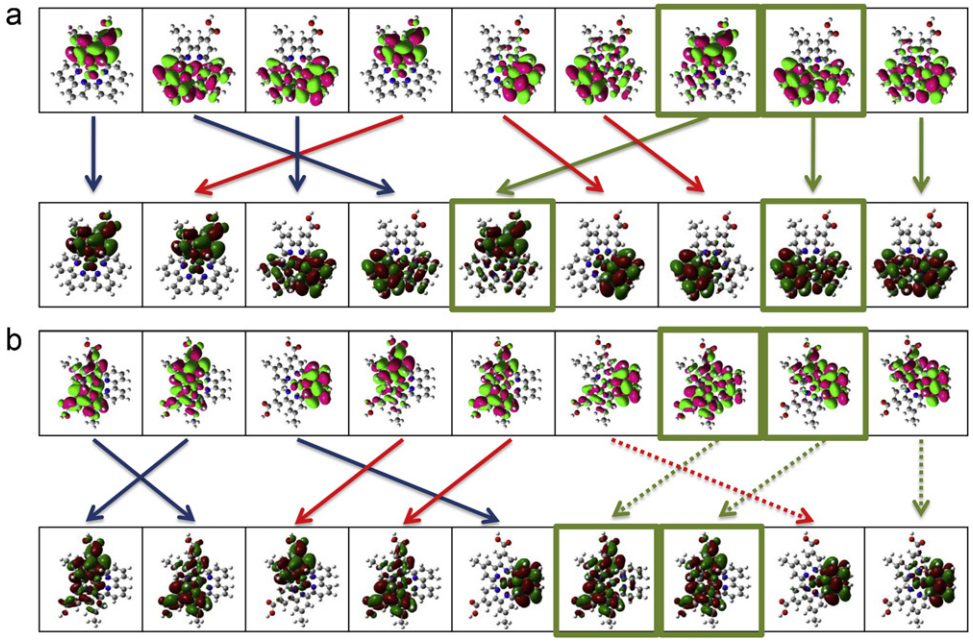

Fig. 4. The first nine unoccupied (electron) transition orbitals (NTOs) in vacuum and in solution for functionalized complexes **C2** (a) and **C3** (b). The top panel for each respective complex represents NTOs obtained from TD-B3LYP calculations in vacuum, while the bottom panel shows their counterparts in solution. The arrows show the redistribution of the Frenkel bands from vacuum to solvent. The colors of the arrows represent bands I (blue), II (red), and III (green). The green squares are around those orbitals with oscillator strength ≥ 0.1. The dashed arrows connect pairs of NTOs which are not exactly alike in vacuum and solvent due to solvent effects. (For interpretation of the references to color in this figure legend, the reader is referred to the web version of this article.)

partly because the primary electron NTOs, which account for all of the behavior of band I (as shown in Section 4.2), are not the only significant contributions to some excited states in solvent bands II and III. If we take those secondary NTOs into account, the resulting orbitals will be a better match with those in vacuum.

The resulting three bands and their parameters are shown in Table 2 for all three complexes in solvent. For the symmetric molecule **C1**, solvent slightly stabilizes all of its excited energies while preserving the structure of the Frenkel bands obtained in vacuum. A small exception is in band I, where the splitting between the three excitations becomes insignificant due to vanishing of the inter-ligand coupling ($s=0$) so that excitation energies of band I are threefold degenerate and equal to Ω (the effective excitation energy of the isolated single ligand). Similar to vacuum, the magnitude of coupling s increases for higher energy bands II and III and has the maximum value for the optically allowed band III for all three complexes. Large transition dipole moments of the two lower-energy excitations in band III result in more delocalized NTOs and stronger inter-ligand coupling. The increase in s also results in a much larger splitting between the transitions for higher energy bands, shown in Fig. 1. Note that the coupling parameter s follows the same sign trends for all complexes as it does in vacuum with the exception of band III for **C3**, which shows a limitation of the model, but does not hinder the general consistency across all parameters.

There is a well noticed trend of significant increase of ε in solvent when compared to those in vacuum. On one hand, large ε leads to a stronger stabilization (when compared to vacuum) of energies of transitions completely or partially localized on mcb ligands, as shown in Fig. 1. On the other hand, increased difference between absolute values of the inter-ligand coupling s and ε leads to a slightly more localized character of transition orbitals in solvent (Fig. 4). Similar to vacuum calculations, two low-energy transitions of band III are optically active and demonstrate stronger delocalization of their transition orbitals over all ligands rather than being localized only on the mcb ligands, as is the case in optically inactive bands I and II. Overall, the Frenkel parameters for all three complexes are virtually as consistent across all three complexes as they are in vacuum.

5. Conclusion

We have demonstrated that a few parameter Frenkel exciton model can accurately and consistently describe optical intensity, localization properties, and splitting patterns of the low-energy excited states of $[Ru(bpy)_3]^{2+}$ as well as of its non-symmetrically functionalized derivatives, $[Ru(bpy)_2(mcb)]^{2+}$ and $[Ru(bpy)(mcb)_2]^{2+}$. Despite the substantial solvatochromism brought by the solvent environment, the model still provides an accurate estimate of the complexes' behavior. In fact, our inter-ligand coupling parameter for $[Ru(bpy)_3]^{2+}$ in vacuum and in solvent is in good agreement with ones obtained from more involved models for this system [16,20,21]. The robustness of the model points to the relative importance of inter-ligand coupling in these Ru(II) complexes in addition to other effects, such as ligand functionalization, solvent, temperature, counter-ions, etc.

Despite its simplicity, results of the Frenkel exciton model provide a better physical interpretation of TDDFT calculations of optical properties of these compounds [39] as well as give a detailed explanation of shifts experimentally observed in absorption spectra of Ru-complexes. In accordance with the model, nine low-energy excitations are combined into three groups (bands) of three, with the two lowest transitions in the third band being optically allowed in all complexes we study. The optical intensity of band III correlates with an increase in the inter-ligand coupling parameter s. This parameter reflects an increase of the transition dipole moments for these excitations. The experimentally observed red-shift in absorption spectra of the complexes functionalized with carboxyl groups is explained by the energy stabilization of the excitations partially localized on the ligands with electron-withdrawing COOH groups. All effects of the energy stabilization and splitting as well as localization properties of the excitation follow directly from a solution of the

relatively simple eigenvalue/eigenvector problem of the Frenkel Hamiltonian.

The behavior of complexes described here has quite a general appearance in transition-metal/multi-ligand dyes and multi-branched polymers [32,33,35,52,53,55,58,75]. Therefore, the physics of photo-excitation in such systems is more linked to the symmetries of the ligand field rather than to particular environmental conditions or elemental constituents of the respective structures. Thus, by applying a simple Frenkel model and by appropriately calibrating the number and types of ligands and the symmetry of the molecule, one can theoretically predict the desired modification required to amplify and tune optical response or other applicable properties of the system.

The complexes described in this work are also a subject of extensive experimental studies in the context of potential applications in photocatalysis and photovoltaic materials based on the quantum dot/Ru-complex interface [8–10,29,30]. In these studies, carboxyl functionalization of anchoring ligands is used to provide a means for chemical and electronic binding of the Ru(II) complexes to the quantum dot. Both the robustness and simplicity of the Frenkel exciton model will allow one to construct reduced parameterized Hamiltonians for a large ensemble of interacting chromophores and simulate photoinduced dynamics in such systems, helping to optimize their efficiency as photo-electrochemical and photo-catalyst agents.

Acknowledgments

VVA acknowledges Kirill A. Velizhanin for insightful advice and fruitful discussions. This work was supported by the U.S. Department of Energy and Los Alamos LDRD funds. Los Alamos National Laboratory is operated by Los Alamos National Security, LLC, for the National Nuclear Security Administration of the U.S. Department of Energy under contract DE-AC52-06NA25396. S.T. acknowledges support of the Center for Advanced Solar Photophysics, an Energy Frontier Research Center funded by the U.S. Department of Energy (DOE), Office of Science, Office of Basic Energy Sciences (BES). We acknowledge the support of the Center for Integrated Nanotechnology (CINT) and the Center for Nonlinear Studies (CNLS).

References

[1] J.N. Demas, A.W. Adamson, J. Am. Chem. Soc. 93 (1971) 1800.
[2] V. Balzani, G. Bergaminia, F. Marchionia, P. Ceroni, Coord. Chem. Rev. 250 (2006) 1254.
[3] F.G. Gao, A.J. Bard, J. Am. Chem. Soc. 122 (2000) 7426.
[4] K.E. Erkkila, D.T. Odom, J.K. Barton, Chem. Rev. 99 (1999) 2777.
[5] L. Zhang, S. Dong, Anal. Chem. 78 (2006) 5119.
[6] M. Graetzel, Nature 414 (2001) 338.
[7] H. Zabri, I. Gillaizeau, C.A. Bignozzi, S. Caramori, M. Charlot, J. Cano-Boquera, F. Odobel, Inorg. Chem. 42 (2003) 6655.
[8] M. Sykora, M.A. Petruska, J. Alstrum-Acevedo, I. Bezel, T.J. Meyer, V.I. Klimov, J. Am. Chem. Soc. 128 (2006) 9984.
[9] I. Mora-Sero, D. Gross, T. Mittereder, A.A. Lutich, A.S. Susha, T. Dittrich, A. Belaidi, R. Caballero, F. Langa, J. Bisquert, et al., Small 6 (2010) 221.
[10] M. Shalom, J. Albero, Z. Tachan, E. Martinez-Ferrero, A. Zaban, E. Palomares, J. Phys. Chem. Lett. 1 (2010) 1134.
[11] M. Hara, C. Waraksa, J. Lean, B. Lewis, T. Mallouk, J. Phys. Chem. A 104 (2000) 5275.
[12] L. Gallagher, S. Serron, X. Wen, B. Hornstein, D. Dattelbaum, J. Schoonover, T. Meyer, Inorg. Chem. 44 (2005) 2089.
[13] J.K. Hurst, Coord. Chem. Rev. 249 (2005) 313.
[14] J.H. Alstrum-Acevedo, M.K. Brennaman, T.J. Meyer, Inorg. Chem. 44 (2005) 6802.
[15] A. Ceulemans, L.G. Vanquickenborne, J. Am. Chem. Soc. 103 (1981) 2238.
[16] J. Ferguson, F. Herren, Chem. Phys. 76 (1983) 45.
[17] E. Kober, T. Meyer, Inorg. Chem. 23 (1984) 3877.
[18] E. Kober, B. Sullivan, T. Meyer, Inorg. Chem. 23 (1984) 2098.
[19] E. Kober, T. Meyer, Inorg. Chem. 22 (1983) 1614.
[20] E. Kober, T. Meyer, Inorg. Chem. 21 (1982) 3967.
[21] C. Daul, E. Baerends, P. Vernooijs, Inorg. Chem. 33 (1994) 3538.
[22] B. Mayoh, P. Day, Theor. Chim. Acta 49 (1978) 259.
[23] C. Daul, J. Weber, Chem. Phys. Lett. 77 (1981) 593.
[24] S.I. Gorelsky, A.B.P. Lever, J. Organomet. Chem. 635 (2001) 187.
[25] S.I. Gorelsky, E.S. Dodsworth, A.B.P. Lever, A.A. Vlcek, Coord. Chem. Rev. 174 (1998) 469.
[26] M.H.V. Huynha, D.M. Dattelbauma, T.J. Meyerb, Coord. Chem. Rev. 249 (2005) 457.
[27] Q. Wang, S.M. Zakeeruddin, M.K. Nazeeruddin, R. Humphry-Baker, M. Graetzel, J. Am. Chem. Soc. 128 (2006) 4446.
[28] K. Tennakone, G. Kumara, I. Kottegoda, K. Wijayantha, V. Perera, J. Phys. D Appl. Phys. 31 (1998) 1492.
[29] S. Sharma, Z. Pillai, P. Kamat, J. Phys. Chem. B 107 (2003) 10088.
[30] C. Burda, S. Link, M.B. Mohamed, M. El-Sayed, J. Chem. Phys. 116 (2002) 3828.
[31] D. Kuang, C. Klein, Z. Zhang, S. Ito, J.-E. Moser, S.M. Zakeeruddin, M. Graetzel, Small 3 (2007) 2094.
[32] T. Minami, S. Tretiak, V. Chernyak, S. Mukamel, J. Lumin. 87–89 (2000) 115.
[33] V. Chernyak, E.Y. Poliakov, S. Tretiak, S. Mukamel, J. Chem. Phys. 111 (1999) 4158.
[34] G.D. Scholes, ACS Nano 2 (2008) 523.
[35] F.C. Spano, Acc. Chem. Res. 43 (2010) 429.
[36] B.P. Krueger, G.D. Scholes, G.R. Fleming, J. Phys. Chem. B 102 (1998) 5378.
[37] D.M. Eisele, J. Knoester, S. Kirstein, J.P. Rabe, D.A.V. Bout, Nat. Nanotechnol. 4 (2009) 658.
[38] S. Tretiak, W.M. Zhang, V. Chernyak, S. Mukamel, Proc. Nat. Acad. Sci. USA 96 (1999) 13003.
[39] E. Badaeva, V.V. Albert, S. Kilina, A. Koposov, M. Sykora, S. Tretiak, Phys. Chem. Chem. Phys. 12 (2010) 8902.
[40] A.S. Davidov, in: Theory of Molecular Excitons, Plenum Press, , 1971.
[41] M. Pope, C.E. Swenberg, Electronic Processes in Organic Crystals, Clarendon Press, Oxford University Press, Oxford, New York, 1982.
[42] G. Wannier, Phys. Rev. 52 (1937) 191.
[43] V. Coropceanu, J. Cornil, D. da Silva Filho, Y. Olivier, R. Silbey, J.-L. Bredas, Chem. Rev. 107 (2007) 926.
[44] K. Ohta, M. Yang, G.R. Fleming, J. Chem. Phys. 115 (2001) 7609.
[45] C. Didraga, J.A. Klugkist, J. Knoester, J. Chem. Phys. B 106 (2002) 11474.
[46] G.P. Bartholomew, M. Rumi, S.J.K. Pond, J.W. Perry, S. Tretiak, G.C. Bazan, J. Am. Chem. Soc. 126 (2004) 11529.
[47] S. Tretiak, C. Middleton, V. Chernyak, S. Mukamel, J. Phys. Chem. B 104 (2000) 4519.
[48] V. Sundström, T. Pullerits, R. van Grondelle, J. Phys. Chem. B 103 (1999) 2327.
[49] X.C. Hu, A. Damjanovic, T. Ritz, K. Schulten, Proc. Nat. Acad. Sci. USA 95 (1998) 5935.
[50] H. Lee, Y.-C. Cheng, G. Fleming, Science 316 (2007) 1462 (ISSN: 0036-8075).
[51] H. Fidder, J. Knoester, D.A. Wiersma, J. Chem. Phys. 95 (1991) 7880.
[52] D.J. Heijs, V.A. Malyshev, J. Knoester, J. Chem. Phys. 121 (2004) 4884.
[53] A. BarHaim, J. Klafter, R. Kopelman, J. Am. Chem. Soc. 119 (1997) 6197.
[54] C. Wu, S.V. Malinin, S. Tretiak, V.Y. Chernyak, Nat. Phys. 2 (2006) 631.
[55] F. Terenziani, C. Katan, E. Badaeva, S. Tretiak, M. Blanchard-Desce, J. Phys. Chem. B 20 (2008) 4641.
[56] C. Katan, S. Tretiak, M.H.V. Werts, A. Bain, R.J. Marsh, N. Leonczek, N. Nicolaou, E. Badaeva, O. Mongin, M. Blanchard-Desce, J. Phys. Chem. B 111 (2007) 9468.
[57] C. Katan, M. Charlot, O. Mongin, C. Le Droumaguet, V. Jouikov, F. Terenziani, E. Badaeva, S. Tretiak, M. Blanchard-Desce, J. Phys. Chem. B 114 (2010) 3152.
[58] C. Katan, F. Terenziani, O. Mongin, M. Werts, L. Porres, T. Pons, J. Mertz, S. Tretiak, M. Blanchard-Desce, J. Phys. Chem. A 109 (2005) 3024.
[59] D. Beljonne, W. Wenseleers, E. Zojer, Z.G. Shuai, H. Vogel, S.J.K. Pond, J.W. Perry, S.R. Marder, J.L. Bredas, Adv. Funct. Mater. 12 (2002) 631.
[60] J.L. Bredas, J.E. Norton, J. Cornil, V. Coropceanu, Acc. Chem. Res. 42 (2009) 1691.
[61] F. C. Spano, private communications, 2010.
[62] M.J. Frisch, G.W. Trucks, H.B. Schlegel, G.E. Scuseria, M.A. Robb, J.R. Cheeseman, G. Scalmani, V. Barone, B. Mennucci, G.A. Petersson, et al., Gaussian 09 Revision A.1, Gaussian Inc., Wallingford, CT, 2009.
[63] V. Barone, M. Cossi, J. Phys. Chem. 102 (1998) 1995.
[64] G. Scalmani, M.J. Frisch, J. Chem. Phys. 123 (2010) 114110.
[65] E. Jakubikova, W. Chen, D.M. Dattelbaum, F.N. Rein, R.C. Rocha, R.L. Martin, E.R. Batista, Inorg. Chem. 48 (2009) 10720.
[66] J.E. Monat, J.H. Rodriguez, J.K. McCusker, J. Phys. Chem. A 106 (2002) 7399.
[67] A. Vlcek, S. Zális, Coord. Chem. Rev. 251 (2007) 258.
[68] M.J. Frisch, G.W. Trucks, H.B. Schlegel, G.E. Scuseria, M.A. Robb, J.R. Cheeseman, J.A. Montgomery Jr., T. Vreven, K.N. Kudin, J.C. Burant, et al., Gaussian 03, Revision D.02, Gaussian, Inc., Wallingford, CT, 2004.
[69] R.L. Martin, J. Chem. Phys. 118 (2003) 4775.
[70] R. Dennington, T. Keith, J. Millam, Gaussview, Version 4.1, Semichem, Inc., Shawnee Mission, KS, 2007.
[71] X.-N. Li, Z.-J. Wu, H.-J. Zhang, X.-J. Liu, L. Zhou, Z.-F. Li, Z.-J. Si, Phys. Chem. Chem. Phys. 11 (2009) 6051.
[72] L. Fodor, G. Lendvay, A. Horváth, J. Phys. Chem. A 111 (2007) 12891.
[73] J. Villegas, S. Stoyanov, W. Huang, D. Rillema, Dalton Trans. (2005) 1042.
[74] S. Fantacci, F. De Angelis, A. Sgamellotti, N. Re, Chem. Phys. Lett. 396 (2004) 43.
[75] I.H. Campbell, D.L. Smith, S. Tretiak, R.L. Martin, C.J. Neef, J.P. Ferraris, Phys. Rev. B 65 (2002) 085210.